

Inkjet Printing of Conductive Inks with High Lateral Resolution on Omniphobic “R^F Paper” for Paper-Based Electronics and MEMS

Joshua Lessing, Ana C. Glavan, S. Brett Walker, Christoph Keplinger, Jennifer A. Lewis,* and George M. Whitesides*

We describe the use of omniphobic “fluoroalkylated paper” (“R^F paper”)^[1] as a substrate for inkjet printing of aqueous inks that are the precursors of electrically conductive patterns. By controlling the surface chemistry of the paper, it is possible to print high resolution, conductive patterns that remain conductive after folding and exposure to common solvents. Inkjet printing on omniphobic paper is a promising method of fabrication for low-cost, flexible, foldable, and disposable conductors on paper (and other flexible substrates) for electronics, microelectromechanical systems (MEMS), displays, and other applications. The ability to resist wetting by liquids with a wide range of surface tensions, combined with foldability, mechanical flexibility, light weight, low cost, and gas permeability, makes omniphobic R^F paper a versatile alternative to the polymer, glass and silicon-based materials upon which printed electronics are currently being deposited.

To make printing the primary platform for patterning flexible conductors, inexpensive functional inks and substrates must be developed and integrated with a fabrication process capable of broad use. Paper, which is both ubiquitous and inexpensive, has been used as a substrate for printed electronics since the 1960s, when Brody and Page at Westinghouse Electric first stencil-printed inorganic thin-film transistors on paper.^[2,3] Despite many advances in the field of printed electronics,^[4–9] including inkjet printing on paper,^[10–14] conventional cellulose-based paper still remains an underutilized substrate in commercial applications other than conventional printing,^[15,16] due, in part, to the poor barrier properties it provides for liquids. Wetting has the effect of dispersing inks deposited on the substrate, and lowering the resolution and conductivity of printed structures. Moreover, since paper is hygroscopic, changes in

ambient humidity can alter the performance of the printed circuit.

Common methods for printing electronics on paper (e.g., gravure, screen printing, stencil printing, chemical vapor deposition with shadow masking)^[15,17] require the creation of a master (a custom-patterned component such as a screen, stencil, or mask) for printing each new pattern. The fabrication of these masters is a time-consuming and often expensive process, which is incompatible with rapid prototyping and mass customization of electronics, although these technologies are widely used in large-scale manufacturing. Russo et al. have recently developed a pen-on-paper approach for fabricating electronic structures on paper;^[18] the resolution of this method is, however, limited to a few hundred microns or higher and the method is not readily scalable.

Here, we report a digital fabrication method for creating high-resolution conductive patterns on paper that both advances the use of paper substrates for printed electronics, and contributes to our program on low-cost, paper-based diagnostics.^[19–31] The major innovation in this work is the use of omniphobic paper^[1] as a substrate for the deposition of multiple inks using a piezoelectric inkjet printer. Piezoelectric inkjet printing is a non-contact, additive, and high-precision printing method (with resolution typically $\geq 20 \mu\text{m}$, though higher resolution has been obtained at the laboratory scale,^[15,32,33] that does not require the generation of a master, but instead creates patterns based on easily modifiable digital files.^[15,34] The precise control over the positioning of the droplets and over the interfacial free energy of the paper substrate enabled us to print, with high resolution, conductive patterns that are resistant to damage from exposure to common solvents and to folding.

We modified the surface free energy of paper using a fast vapor-phase treatment with organosilanes.^[1] This process, which occurs in approximately five minutes, does not require wetting (and distorting) the paper, or removal of solvents. Treatment with non-fluorinated organosilanes renders paper hydrophobic; treatment with highly fluorinated compounds such as fluoroalkyltrichlorosilanes transforms paper into a material that is omniphobic (both hydrophobic and oleophobic).^[1] In both cases, the chemical modifications result in engineered papers with mechanical properties independent of humidity. These engineered papers still retain the flexibility and low resistance to gas transport of untreated paper.^[1]

We used four commercially available reagents to study the effect of the change in interfacial free energy (provided by the covalently grafted organosilane) on the resolution of printed

Dr. J. Lessing, A. C. Glavan, Dr. C. Keplinger,
Prof. G. M. Whitesides
Department of Chemistry and Chemical Biology
Harvard University
12 Oxford Street, Cambridge, MA 02138, USA
E-mail: gwhitesides@gmwhgroup.harvard.edu

Dr. S. B. Walker, Prof. J. A. Lewis, Prof. G. M. Whitesides
Wyss Institute for Biologically Inspired Engineering
Harvard University
3 Blackfan Circle, Boston, MA 02115, USA
E-mail: jalewis@seas.harvard.edu

Dr. S. B. Walker, Prof. J. A. Lewis
Harvard School of Engineering and Applied Sciences
29 Oxford Street, Cambridge, MA 02138, USA



DOI: 10.1002/adma.201401053

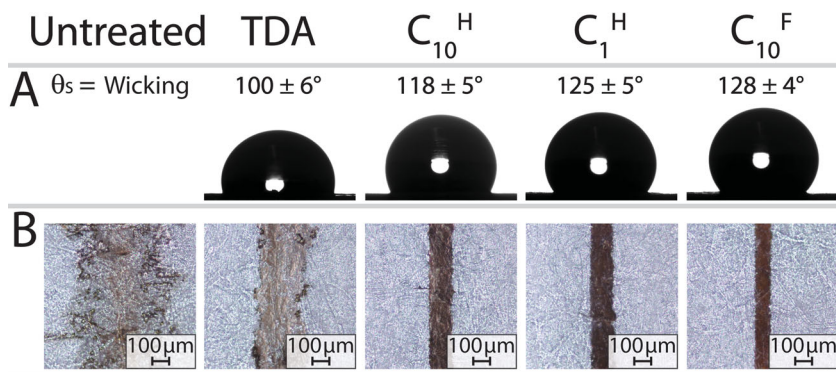


Figure 1. (A) Images of 10- μL drops of water on a series of Canson tracing papers, modified with different organosilanes, and their corresponding static contact angles (θ_s) (with standard deviation for $n = 7$ measurements). (B) Optical micrographs of silver wires printed on the modified or unmodified Canson tracing paper substrates using the reactive silver ink with a target resolution of 80 μm .

conductive features: (i) (3,3,4,4,5,5,6,6,7,7,8,8,9,9,10,10,10-heptafluorodecyl) trichlorosilane ($\text{CF}_3(\text{CF}_2)_7\text{CH}_2\text{CH}_2\text{SiCl}_3$, “C₁₀^F”), (ii) methyltrichlorosilane (CH_3SiCl_3 , “C₁^H”), (iii) decyltrichlorosilane ($\text{CH}_3(\text{CH}_2)_9\text{SiCl}_3$, “C₁₀^H”), and (iv) tris(dimethylamino)silane (TDA). A relatively smooth paper, (Canson tracing paper, Model No. 702–321) is used as a substrate for applications requiring maximum lateral resolution; this choice of paper minimizes irregularities in the conductivity and resolution of printed features induced by surface roughness.

We first examined, by means of apparent static (θ_s) contact angle^[35] measurements, the wettability of the organosilane-modified paper substrates.^[1] In the absence of this treatment, water droplets are found to immediately wick into the paper (Figure 1). By contrast, silanization renders the papers hydrophobic, i.e., water no longer wicks into them, but rather forms droplets on their surfaces with apparent static contact angles, $\theta_s^{\text{H}_2\text{O}}$, between $100^\circ \pm 6$ (for TDA, $n = 7$) and $128^\circ \pm 4$ (for C₁₀^F, $n = 7$). Based on the static contact angle measurements, the hydrophobicity of the surfaces appears to increase according to the series: untreated paper < TDA < C₁₀^H < C₁^H < C₁₀^F.

Figure 1 clearly demonstrates that the wetting of untreated and silanized paper by water correlates with the lateral resolution of the printed conductive features. Canson tracing paper, untreated or silanized with TDA, C₁^H, C₁₀^H, and C₁₀^F, is used as a substrate for the inkjet printing of 80- μm -wide wires (the intended width based on the features in the digital file) using reactive silver ink dispensed by a Fuji Dimatix DMP-2831 printer (see Supplementary Information for details). We used this reactive silver ink^[36] because it yields patterned features whose electrical conductivity is superior to that of features obtained using commercial silver nanoparticle inks. The reactive silver ink is essentially a modified Tollens' reagent: that is, an aqueous solution that contains a soluble complex of silver ions, primary amines and a reducing agent—formic acid. As the chelating primary amines are volatilized upon heating at modest temperatures ($\leq 120^\circ\text{C}$), the formic acid reduces the uncomplexed silver ions to silver particles.

This process results in patterned features with conductivities that are 60–90% of the bulk conductivity of silver, since there

are no polymeric or other organic residues in the ink formulation.^[36] Optical micrographs show that the lateral resolution of printed features improves with increasing hydrophobicity: untreated paper = $585 \pm 87 \mu\text{m}$, TDA = $292 \pm 34 \mu\text{m}$, C₁₀^H = $149 \pm 31 \mu\text{m}$, C₁^H = $137 \pm 13 \mu\text{m}$, and C₁₀^F = $90 \pm 5 \mu\text{m}$ ($n = 10$ measurements of the feature width). The lateral resolution of the printed features is linearly correlated with the apparent static contact angle, $\theta_s^{\text{H}_2\text{O}}$ on the surface of each paper (Figure S1). This effect is most pronounced for C₁₀^F-treated paper, which shows a substantial improvement in maximum lateral resolution compared to the untreated paper substrate. Scanning electron microscopy (Figure S2), energy-dispersive X-ray spectroscopy (Figure S3), and optical profilometry (Figure S4) reveal that the hydro-

phobicity of the engineered paper surfaces serves to focus the deposition of silver particles onto a smaller area, thus enabling printing of conductive features. The resistance per unit length of the printed wires in Figure 1 decreases with increasing hydrophobicity: $R^{\text{TDA}} = 2371 \pm 1618 \Omega/\text{cm}$, $R^{\text{C}_{10}^{\text{H}}} = 400 \pm 206 \Omega/\text{cm}$, $R^{\text{C}_{1}^{\text{H}}} = 265 \pm 64 \Omega/\text{cm}$, and $R^{\text{C}_{10}^{\text{F}}} = 132 \pm 25 \Omega/\text{cm}$ (each resistances measured for $n = 7$ distinct features). The observed conductivity of wires printed on silanized papers stands in contrast with the very high resistance of the features printed on untreated paper (resistance greater than the detection limit of our multimeter $>10 \text{ M}\Omega$).

The resolution of inkjet-printed patterns is limited by several factors: the wettability of the substrate, the hydrodynamics of the jetted microdroplets, and the volatility of the constituents of the ink.^[34] Typically, 20 μm is considered the smallest feature size achievable via inkjet printing.^[37] Features of this size are typically achieved using 1-pL droplets, but can also be achieved by tuning the waveform of 10-pL cartridges to generate droplet volumes below 10 pL. We chose our most hydrophobic paper in the series, Canson tracing paper treated with C₁₀^F ($\theta_s^{\text{H}_2\text{O}} = 129^\circ \pm 4$, $n = 7$), to test the maximum lateral resolution achievable using reactive silver ink dispensed from a 10-pL Dimatix cartridge. A 10-pL spherical droplet has a diameter of 27 μm . We printed lines with thickness determined by the width of single drops, with a spacing set at 20 μm between consecutive drops. SEM imaging (Figure S5) shows that a maximum lateral resolution of $28 \pm 5 \mu\text{m}$ and a line edge roughness of 6 μm is achieved on this paper. To the best of our knowledge, this resolution has never before been achieved with droplets of this volume, suggesting that a high level of control over line width can be achieved by decreasing the surface free energy of the substrate. Although the 28 μm -wide feature appears to be continuous by SEM, it is not conductive. Since its width is on the same size scale as that of the individual cellulose fibers, the surface roughness of the tracing paper likely introduces local discontinuities in the patterned wires (see Figure S4). These discontinuities could be remedied simply by printing multiple overlapping layers of ink. Unfortunately, we are unable to demonstrate this effect because our printer cannot achieve accurate multilayer printing at this scale due to its inability to

reproduce droplet location below an accuracy of $\pm 25 \mu\text{m}$. We anticipate that printing of microscopic wires ($< 30 \mu\text{m}$) with a 10-pL droplet would be possible by using a printer with higher droplet-positioning accuracy and a paper with lower surface roughness (e.g., nanocellulose paper).^[38]

To test the performance of the inkjet-printed silver features upon exposure to common solvents, we quantified the change in electric resistance of silver wires printed on C_{10}^F paper after drops of solvent are deposited on their surface. Ten 50- μL drops of solvent were deposited along the path of each silver wire ($n = 7$, 10 cm-long, and 1 mm-wide wires were tested per solvent). We found that the percentage change in resistance after 30 min of solvent exposure is negligible for conventional solvents used for inkjet printing (e.g., water, ethanol, and glycerin). We also tested a chemically diverse set of solvents (toluene, glacial acetic acid, chloroform, dimethyl sulfoxide, acetone, and hexadecane) that are not conventionally used for inkjet printing and again found that only a small change in resistance occurred (Figure S6).

To compare the performance conferred by different substrates to high-conductivity features, we printed wires (25 cm long, and 120 μm wide, printed with 5 layers of ink) of silver nanoparticle-, reactive silver-,^[36] and carbon-based inks onto a series of “alkylated papers” (“ R^H paper” produced by vapor-phase silanization of paper with alkyl trichlorosilanes), “fluoroalkylated papers” (“ R^F paper” produced by vapor-phase silanization of paper with fluoroalkyl trichlorosilanes), and PET films, and tested their resistance. When using the same ink, wires printed on C_{10}^F and C_1^H treated paper have resistances comparable to wires printed on a commercial PET film designed for conductive inkjet printing (see Table 1).

To investigate the mechanical flexibility and resistance to creasing of the printed silver features, we produced a linear array of them ($n = 7$ distinct samples of paper, each with printed wire arrays were tested) with width = 1 mm, and length = 10 cm, spaced 3 mm apart, using a single layer of reactive silver ink on Canson C_{10}^F -treated tracing paper. We measured the resistance of a feature as a function of the number of times we creased the sheet of paper on which they were printed. One cycle constituted folding the paper to a full crease –corresponding to the formation of a -180° angle (acute folding, silver on the inside) or a $+180^\circ$ angle (obtuse folding, silver on the outside) –and back. The ends of the electrode-patterned paper substrates are affixed to the crossheads of an Instron

5544A electromechanical testing machine, and the distance between the crossheads is cycled between 0 and 40 mm. Images of these samples undergoing a creasing cycle are shown in Figure S7 A-C. A crosshead distance of 0 mm leads to the formation of a crease in the paper substrate in the direction perpendicular to the printed silver features. Figure S7D shows the averaged resistance values obtained from the array as a function of the number of creasing cycles. The resistance of the features did not vary significantly ($< 5\%$) from the original, pre-creasing resistance, after being folded once to either a $+180^\circ$ or a -180° angle. This observation remains true for 100 consecutive folds, i.e., there is no significant increase ($< 5\%$) in the respective electrical resistance of the prints relative to their initial pre-creased values. We hypothesize that the resilience of the wires to repeated cycles of folding is due, in part, to the strength of adhesion of the silver to the cellulose fibers of the C_{10}^F paper, as evidenced by the adhesion test in Movie M1.

Electroadhesion. As a demonstration of the ability to print defect-free high-resolution conductive features over large areas, we prototyped flexible electroadhesive devices on omniphobic R^F tracing paper, using inkjet printing. Electroadhesion^[39] is an electrically controlled adhesion technology used for applications that require reversible, adhesive-free, binding to a substrate.^[40–45] A typical electroadhesion pad consists of two interdigitated electrodes patterned on the surface of a dielectric material. Electrostatic forces are created between electroadhesive pads and a substrate that is either electrically insulating or conductive (although much lower forces are achieved with electroadhesion for nonconducting objects).^[42] Charging the interdigitated electrode creates fringe field lines between the positive and negative electrodes that extend in the direction normal to the electrode pattern. When the electroadhesive pad is brought in proximity to a substrate (e.g., glass, drywall, wood, concrete, or metals), its fringe-field lines penetrate the substrate, and redistribute charge to create a pattern of opposite polarity in the substrate.^[39–42] The Coulombic attraction between the charges on the electrode and the complementary, induced charges on the surface of the substrate creates an electrostatic force that can be used to adhere the electroadhesive pad to the substrate. Controlling of the electrostatic adhesion voltage permits the adhesion to be turned on and off easily.

We used inkjet printing of the reactive silver ink to deposit a pair of interdigitated electrodes on a flexible dielectric layer (C_{10}^F -treated Canson tracing paper), in order to fabricate an electroadhesive device (Figure 2). The high resolution of the printing in conjunction with the use of omniphobic paper allowed us to deposit 500- μm wide interdigitated electrodes over a large area (57.5 cm^2). This high resolution of printing resulted in a pattern that was free of defects that give rise to short circuits, which, if present, would render the device inoperable. We note that if the same pattern were inkjet printed on untreated paper, the bleeding of reactive silver ink features into one another would result in short circuits. We applied a potential difference of 2 kV by connecting the electrodes to a high voltage power supply, and subsequently observed adhesion of the device to a glass surface that was sufficient to support a 500-g weight hanging from the base of the sheet (Movie M2).

To demonstrate the utility of omniphobic R^F paper as a substrate for creating printed electronics, we fabricated mechanical

Table 1. Comparison between resistances (Ω) of wires^{a)} ($n = 10$) printed on different substrates—modified papers (C_1^H and C_{10}^F) and a PET film—using three different inks.

Ink tested	$R_{C_1^H}$ [Ω]	$R_{C_{10}^F}$ [Ω]	R_{PET} [Ω] ^{e)}
Reactive Silver Ink ^{b)}	5 ± 1	4 ± 1	13 ± 1
Silver Nano-particle Ink ^{c)}	24 ± 3	10 ± 4	33 ± 7
Carbon Ink ($\times 10^{-4}$) ^{d)}	87 ± 1	76 ± 2	65 ± 7

^{a)} 25 cm \times 120 μm wires were printed in 5 layers; ^{b)} Reactive Ag Ink #1 (Electroninks Inc.), ^{c)} Nanoparticle Colloidal Silver Ink DGP 40-LT-15C (Advanced Nano Products), ^{d)} Carbon Ink 3801 (Methode Electronics Ink); ^{e)} PET film (DuPont Melinex ST506/500).

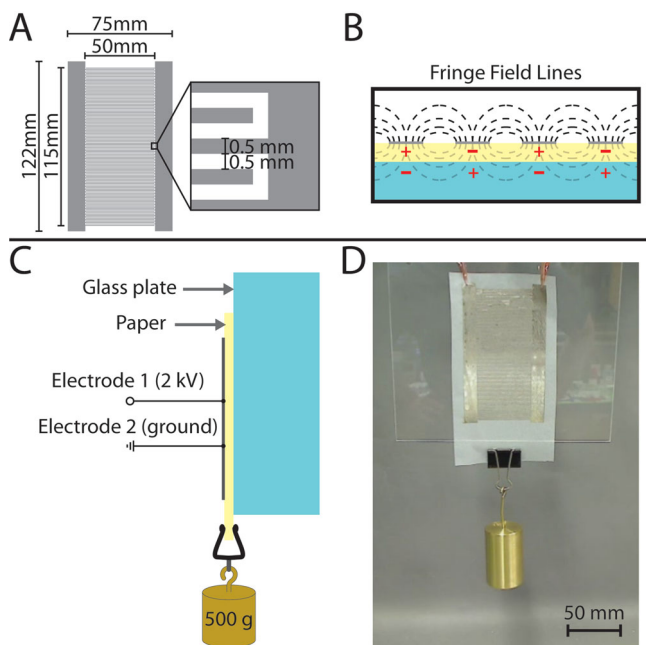


Figure 2. Electroadhesive pad printed on C_{10}^F Canson tracing paper using the reactive silver ink. (A) Schematic of the interdigitated electrode design used for the pad. (B) Illustration of a cross-section of the electroadhesive pad depicting the fringe electric field lines, generated from the electrode, charging a glass surface by induction. (C) Schematic showing the arrangement of the electroadhesive pad used for the experiment. (D) An electroadhesive pad (with dimensions given in A) under an applied 2 kV potential adheres to a glass plate with sufficient strength to support a 500 g weight.

and electrochemical sensors with carbon ink on C_{10}^F modified paper. We used carbon ink for the demonstration of paper-based MEMS and electrochemical devices in order to achieve a larger resistivity and a broader electrochemical window, respectively, than possible with silver inks. MEMS deflection sensors were fabricated to demonstrate an application in flexible electronics; electrochemical testing strips demonstrated an application that requires solvent-resistant electronics.

Paper MEMS. We fabricated cantilever-type MEMS deflection sensors by depositing carbon ink (Methode 3801) on C_{10}^F -treated Canson Vellum paper. Canson Vellum paper (Model No. 702–442) is used as a substrate for the printing of MEMS cantilever deflection sensors, because it has a higher bending elastic modulus than many other papers. We tested the ability of a series ($n = 5$) of these sensors (Figure 3A – left) to measure beam deflection by cycling the device between an upward and downward deflection point while measuring the end-to-end resistance of the printed cantilever. An image and a schematic of the testing rig are shown in Figure 3A (right) and 3B respectively. The plot in Figure 3C shows the resistance as a function of time for a typical device, as it is deflected cyclically. We observed a drop in resistance upon compression of the print during upward deflection, reflecting (we hypothesize) an increase in the number of connections in the percolation network between carbon particles. A rise in resistance is observed during downward deflection as a result of a

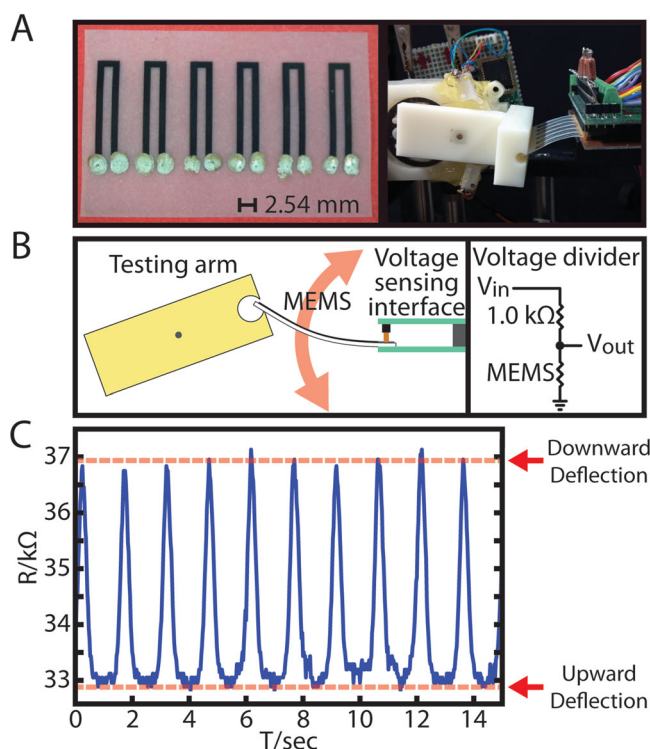


Figure 3. (A) Left, MEMS deflection sensor fabricated by depositing carbon ink on C_{10}^F Canson Vellum paper with an inkjet printer. Ercon 3456 silver ink was applied manually at the ends of the device to improve electrical connections with the testing rig. Right, Image of the experimental setup used for cyclically deflecting an array ($n = 5$) of MEMS sensors. (B) Schematic describing the experimental setup (left) and a diagram of the circuit employed for measuring device resistances (right). (C) Plot of resistance vs. time for a representative device during 10 cycles of upward/downward deflection.

corresponding decrease in the number of connections upon extension.

Paper-Based Electrodes. We used inkjet printing to deposit arrays of electrodes over a non-planar paper surface consisting of wells embossed in omniphobic C_{10}^F paper. Whatman #1 Chromatography Paper is used as a substrate for the printing of electrodes in electrochemical devices, because its high surface roughness increased the surface area accessible for electrochemical reactions and, for some applications, the sensitivity of detection. The electrode configuration consists of inkjet-printed working, counter, and quasi-reference carbon electrodes (WE, CE, and QRE, respectively). A well-defined area for the electrolyte/analyte solution is formed by partially overlapping the electrode area over an embossed well (Figure 4A–D). The electrochemical operation of the paper-based three-electrode system is tested by recording cyclic voltammograms for 1 mM and 100 μ M solutions of 4-aminophenol^[46] (Figure 4E). The precise control over the positioning and volume of the droplets afforded by inkjet printing enabled us to print electrodes with a coefficient of variation as low as 2.1%, measured as the relative standard deviation (RSD, defined as the percentage ratio of the standard deviation to the mean of the distribution) in the peak anodic current

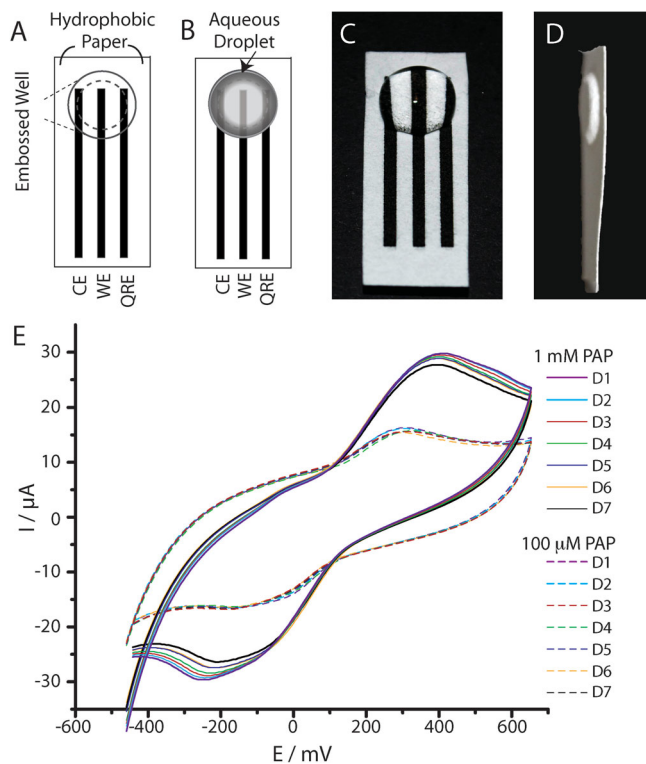


Figure 4. The reproducibility of electrodes, printed on embossed omniphobic C_{10}^F Whatman paper using carbon ink, as characterized by cyclic voltammetry. (A) Design of an electroanalytical device with a three-electrode system. The dotted line indicates that the embossed well is recessed into the surface and protrudes on the back side of the paper. (B) Illustration of the electroanalytical device with a drop placed in the embossed well. (C) Top view of an actual device with a 50- μ L drop of an aqueous solution of an electroactive species added to the well. (D) Side view. (E) Cyclic voltammograms of 4-aminophenol (PAP) at concentrations of 1 mM (solid lines) and 100 μ M (dashed lines) tested on seven different devices (D1–D7). Potential measured vs. the quasi-reference electrode. Scan rate, 100 mV/s.

(i_p , measured from the decaying cathodic current as a baseline,^[47] among different devices.

In summary, we describe the use of inkjet printing to fabricate simple, flexible electronic devices on omniphobic R^F paper. These structures are thin, lightweight, breathable (permeable to gases), and resistant to damage by exposure to water and other common solvents. Unlike electronic systems fabricated on silicon, glass, ceramics or polymers, these structures can be folded and unfolded repeatedly, for storage in small spaces or to form three-dimensional structures, which can be trimmed or shaped using scissors. Moreover, electronics printed on omniphobic R^F paper can be disposed of by incineration thereby reducing environmental issues associated with the storage and management of electronic waste (end-of-life electronics). Our paper-based digital fabrication method has the potential to reduce the cost of development of electrical, electroanalytical and MEMS devices. In addition to use in health monitoring and diagnostics solutions in the developing world, these low-cost, high-performance electronics may find commercial applications in economies in which cost is critically important.

Supporting Information

Supporting Information is available from the Wiley Online Library or from the website of the Whitesides group (<http://gmwgroup.harvard.edu/pubs>).

Acknowledgements

Collaborative aspects of this work (JAL and GMW) were supported by the NSF Materials Research and Engineering Center (award DMR-0820484). Other work (GMW) was funded in part by the Bill & Melinda Gates Foundation (award 51308) and (JAL) the Office of Naval Research through the Multi-University Research Initiative (MURI award N00014-11-1-0690). Optical profilometry, scanning electron microscopy, and energy dispersive x-ray spectroscopy were performed at the Harvard University Center for Nanoscale Systems (CNS), a member of the National Nanotechnology Infrastructure Network (NNIN), which is supported by the NSF (under award ECS-0335765). In particular we would like to thank Nicholas Antoniou, Brittany Gelfand, Mac Hathaway, Andrew Magyar, Carolyn Marks, and Jason Tresback of CNS for their help with data collection. WowWee Group Limited (Hong Kong) and James B. MacArthur from the Harvard University, Department of Physics, assisted in the construction of the MEMS cyclic fatigue-testing device. S.B. Walker gratefully acknowledges support through an IC Postdoctoral Fellowship.

Received: March 6, 2014

Revised: April 9, 2014

Published online: May 30, 2014

- [1] A. C. Glavan, R. V. Martinez, A. B. Subramaniam, H. J. Yoon, R. M. D. Nunes, H. Lange, M. M. Thuo, G. M. Whitesides, *Adv. Funct. Mater.* **2013** DOI: 10.1002/adfm.201300780.
- [2] W. S. Bacon, *Pop Science* **1968**, 193, 124.
- [3] T. P. Brody, *IEEE Trans. Electron Devices* **1984**, 31, 1614.
- [4] A. C. Siegel, S. T. Phillips, M. D. Dickey, N. Lu, Z. Suo, G. M. Whitesides, *Adv. Funct. Mater.* **2010**, 20, 28.
- [5] R. Martins, I. Ferreira, E. Fortunato, *Phys. Status Solidi RRL* **2011**, 5, 332.
- [6] L. Hu, H. Wu, F. La Mantia, Y. Yang, Y. Cui, *ACS Nano* **2010**, 4, 5843.
- [7] D.-H. Kim, Y.-S. Kim, J. Wu, Z. Liu, J. Song, H.-S. Kim, Y. Y. Huang, K.-C. Hwang, J. A. Rogers, *Adv. Mater.* **2009**, 21, 3703.
- [8] U. Zschieschang, T. Yamamoto, K. Takimiya, H. Kuwabara, M. Ikeda, T. Sekitani, T. Someya, H. Klauk, *Adv. Mater.* **2011**, 23, 654.
- [9] M. C. Barr, J. A. Rowehl, R. R. Lunt, J. Xu, A. Wang, C. M. Boyce, S. G. Im, V. Bulović, K. K. Gleason, *Adv. Mater.* **2011**, 23, 3500.
- [10] O.-S. Kwon, H. Kim, H. Ko, J. Lee, B. Lee, C.-H. Jung, J.-H. Choi, K. Shin, *Carbon* **2013**, 58, 116.
- [11] A. Määttänen, P. Ihalainen, P. Pulkkinen, S. Wang, H. Tenhu, J. Peltonen, *ACS Appl. Mater. Inter.* **2012**, 4, 955.
- [12] S. Glatzel, Z. Schnepf, C. Giordano, *Angew. Chem. Int. Ed.* **2013**, 52, 2355.
- [13] P. Ihalainen, F. Pettersson, M. Pesonen, T. Viitala, A. Maattanen, R. Osterbacka, J. Peltonen, *Nanotechnology* **2014**, 25.
- [14] H. Ko, J. Lee, Y. Kim, B. Lee, C.-H. Jung, J.-H. Choi, O.-S. Kwon, K. Shin, *Adv. Mater.* **2014**, n/a.
- [15] D. Tobjork, R. Osterbacka, *Adv. Mater.* **2011**, 23, 1935.
- [16] G. Chinga-Carrasco, D. Tobjork, R. Osterbacka, *J. Nanopart. Res.* **2012**, 14.

- [17] F. Eder, H. Klauk, M. Halik, U. Zschieschang, G. Schmid, C. Dehm, *Appl. Phys. Lett.* **2004**, *84*, 2673.
- [18] A. Russo, B. Y. Ahn, J. J. Adams, E. B. Duoss, J. T. Bernhard, J. A. Lewis, *Adv. Mater.* **2011**, *23*, 3426.
- [19] A. W. Martinez, *Bioanalysis* **2011**, *3*, 2589.
- [20] A. W. Martinez, S. T. Phillips, M. J. Butte, G. M. Whitesides, *Angew. Chem.* **2007**, *46*, 1318.
- [21] A. W. Martinez, S. T. Phillips, E. Carrilho, S. W. Thomas, H. Sindi, G. M. Whitesides, *Anal. Chem.* **2008**, *80*, 3699.
- [22] A. W. Martinez, S. T. Phillips, Z. Nie, C. M. Cheng, E. Carrilho, B. J. Wiley, G. M. Whitesides, *Lab Chip* **2010**, *10*, 2499.
- [23] A. W. Martinez, S. T. Phillips, G. M. Whitesides, *Proc. Natl. Acad. Sci. U. S. A.* **2008**, *105*, 19606.
- [24] A. W. Martinez, S. T. Phillips, G. M. Whitesides, E. Carrilho, *Anal. Chem.* **2010**, *82*, 3.
- [25] A. W. Martinez, S. T. Phillips, B. J. Wiley, M. Gupta, G. M. Whitesides, *Lab Chip* **2008**, *8*, 2146.
- [26] E. Carrilho, S. T. Phillips, S. J. Vella, A. W. Martinez, G. M. Whitesides, *Anal. Chem.* **2009**, *81*, 5990.
- [27] S. A. Klasner, A. K. Price, K. W. Hoeman, R. S. Wilson, K. J. Bell, C. T. Culbertson, *Anal. Bioanal. Chem.* **2010**, *397*, 1821.
- [28] E. Fu, P. Kauffman, B. Lutz, P. Yager, *Sens. Actuators, B* **2010**, *149*, 325.
- [29] L. Ge, S. M. Wang, X. R. Song, S. G. Ge, J. H. Yu, *Lab Chip* **2012**, *12*, 3150.
- [30] H. Liu, X. Li, R. M. Crooks, *Anal. Chem.* **2013**, *85*, 4263.
- [31] K. Scida, B. L. Li, A. D. Ellington, R. M. Crooks, *Anal. Chem.* **2013**, *85*, 9713.
- [32] T. Sekitani, Y. Noguchi, U. Zschieschang, H. Klauk, T. Someya, *Proc. Natl. Acad. Sci. USA* **2008**, *105*, 4976.
- [33] C. W. Sele, T. von Werne, R. H. Friend, H. Sirringhaus, *Adv. Mater.* **2005**, *17*, 997.
- [34] M. Singh, H. M. Haverinen, P. Dhagat, G. E. Jabbour, *Adv. Mater.* **2010**, *22*, 673.
- [35] A. W. Adamson, A. P. U. Gast, *Physical Chemistry of Surfaces*, 6th ed., Wiley, **1997**.
- [36] S. B. Walker, J. A. Lewis, *J. Am. Chem. Soc.* **2012**, *134*, 1419.
- [37] S. H. Ko, H. Pan, C. P. Grigoropoulos, J. M. J. Frechet, C. K. Luscombe, D. Poulidakos, *Appl. Phys. A: Mater. Sci. Process.* **2008**, *92*, 579.
- [38] I. Siro, D. Plackett, *Cellulose* **2010**, *17*, 459.
- [39] G. J. Monkman, P. M. Taylor, G. J. Farnworth, *Int. J. Cloth. Sci. Tech.* **1989**, *1*, 14.
- [40] G. Monkman, *Ind. Robot* **2003**, *30*, 326.
- [41] G. J. Monkman, *Robotica* **1992**, *10*, 183.
- [42] G. J. Monkman, *Int. J. Robot. Res.* **1997**, *16*, 1.
- [43] H. Prahlad, R. Pelrine, S. Stanford, J. Marlow, R. Kornbluh, *IEEE Int. Conf. Robot. Autom.* **2008**, *1–9*, 3028.
- [44] H. Prashad, *Trans. ASME. J. Tribol.* **1988**, *110*, 448.
- [45] H. Q. Wang, A. Yamamoto, T. Higuchi, *IEEE Int. Conf. Robot. Autom.* **2012**, 914.
- [46] O. Niwa, Y. Xu, H. B. Halsall, W. R. Heineman, *Anal. Chem.* **1993**, *65*, 1559.
- [47] A. J. Bard, L. R. Faulkner, *Electrochemical Methods*, 2nd ed., John Wiley & Sons, New York **2001**.